ACS Sustainable Chemistry & Engineering

Research Article

pubs.acs.org/journal/ascecg

Tunable Solvent Permeation Properties of Thin Film Nanocomposite Membrane by Constructing Dual-Pathways Using Cyclodextrins for Organic Solvent Nanofiltration

Heng Mao,[†] Haoqing Zhang,[†] Yifan Li,[†] Yubin Xue,[†] Fei Pei,[‡] Jingtao Wang,*[,†] and Jindun Liu[†]

[†]School of Chemical Engineering and Energy, Zhengzhou University, Zhengzhou 450001, People's Republic of China

[‡]Pen-Tung Sah Institute of Micro-Nano Science and Technology, Xiamen University, Xiamen 361005, People's Republic of China

Supporting Information

ABSTRACT: Design and fabrication of thin film nanocomposite (TFN) membranes with tunable solvent permeation properties is highly required to meet the demands of practical applications. Herein, a series of TFN membranes are elaborately fabricated by embedding cyclodextrins (CDs) into hydrophilic polymeric membrane (e.g., polyethylenimine, PEI). Within the active layer, hydrophobic cavities of CDs serve as exquisite pathways for nonpolar solvents, whereas the free volume cavities of the PEI matrix act as efficient pathways for polar solvents, constructing a dual-pathway nanostructure. The solvent permeation properties of these two pathways can be accurately tuned by adjusting the cavity size of CD and the fractional free volume (FFV) of PEI. Increasing the cavity size of CD allows larger nonpolar solvent to permeate, meanwhile increasing solvent flux. For instance, varying the cavity size from 0.60 to 0.75 nm elevates the toluene (0.60 nm) permeance from 0.13 to 2.52 L m^{-2} h^{-1} bar $^{-1}$. Similar behaviors are observed for polar solvents when increasing the FFV of PEI by adjusting the PEI−CD interfacial interactions. Particularly, the isopropyl alcohol permeance is elevated from 3.37 to 4.16 L m^{-2} h^{-1} bar $^{-1}$ when increasing FFV from 0.489% to 0.502%. Moreover, the rejection ability and extended trial of TFN membranes are also explored.

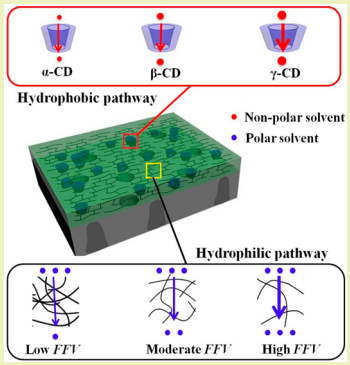

KEYWORDS: *Cyclodextrin, Thin film nanocomposite membrane, Interfacial polymerization, Tunable solvent permeation properties, Organic solvent nanofiltration*

INTRODUCTION

The thin film nanocomposite (TFN) membrane has triggered increasing attention due to the expectation that its unique structure can bring amazing improvement in several fields such as desalination, pervaporation, gas separation, etc.[1−3] They are usually synthesized by incorporating nanofillers (e.g., silica, zeolite) within the ultrathin active layer of a thin film composite membrane. The layered architecture endows the TFN membrane with the optimal performances for target applications, as the two layers can be independently modulated. Recently, the TFN membrane has evolved as an enthusiastic concern in the field of organic solvent nanofiltration (OSN). Random discharge of organic solvents has caused terrible safety, environmental, and economic impacts. Therefore, various approaches are used to separate and recycle organic solvents. Because of the inherent simplicity, energy efficiency, and modular nature, OSN is a sustainable technology for the separation of solutes, solvent exchange, and solvent recovery. The environmental burden of OSN to process organic solvents is less than that of alternative technologies (i.e., distillation, or extraction), and even greener than other downstream processing technologies.[4,5] Meanwhile, OSN can effectively separate molecules or nanoparticles (Mw, 200−1000 Da) within organic media by applying simply a pressure gradient.[6−8] In general, the solvent systems in practical applications are sophisticated, containing both nonpolar and polar solvents. Unfortunately, most commercial OSN membranes are mainly suitable for either nonpolar or polar solvents, and usually have the intrinsic trade-off effect between permeability and rejection.[9,10] The development of the OSN membrane is urgently required to attain tunable solvent permeation properties in a wide range of organic solvents. Clearly, the TFN OSN membrane will become an alternative candidate to address these daunting hurdles.

Previous studies have demonstated that the transfer properties of TFN OSN membranes are mainly determined by the microstructure and inherent packing of polymer chains.[10,11] Recently, novel TFN membranes have been developed by embedding a dispersed phase of particles into the polymeric matrix, combining the advantages of polymeric membranes (processability, robustness, inexpensive) with the stable separation performance of inorganic nanofillers.[12,13] Specifically, Peyravi et al. reported that the incorporation of inorganic nanofillers provided distinct nanodomains along their interfaces, regulating the migration of solvent and lengthening the transfer pathway for solute.[14] Meanwhile, the inorganic

Received: January 30, 2015
Revised: July 30, 2015
Published: August 6, 2015

DOI: 10.1021/acssuschemeng.5b00435
ACS Sustainable Chem. Eng. 2015, 3, 1925−1933

nanofillers could further interfere the chain packing and enlarged the free volume cavities of the polymer matrix, benefiting for low solvent transporting resistance.[15,16] Exemplarily, free volume characteristics can reflect mathematically the mobility and packing of polymer chains, in turn describing the internal morphology of the membrane. Because the transport properties of the TFN membrane are strongly dependent on its interfacial morphology, a deeper understanding is required urgently about the effects of the inorganic nanofillers on the free volume characteristics of membrane. For instance, the large free volume can afford high permeability but low rejection to the membrane, and vice versa. In addition, the rejection ability of the TFN membrane incorporated by nanofillers may be raised since the excellent compatibility between inorganic nanofillers and polymer matrix, affording the extended diffusion pathways for solute.[17,18] Accordingly, the separation performances of TFN membrane are improved. Most recently, Sorribas et al. prepared the TFN OSN membranes incorporating with MOFs within the active layer, and the membranes displayed an exceptional increase in permeability from 1.7 to 11.1 L m^{-2} h^{-1} bar^{-1} for THF/PS.[19] Peyravi et al. reported a high methanol flux and good dye rejection by introducing TiO_2 nanoparticles into the polyethylenimine (PEI) active layer.[14] However, the up-scaling preparation of the TFN membrane is still not straightforward due to the following main disadvantages: (i) many inorganic nanofillers tend to aggregate, derived from the strong surface tension and weak affinity with polymer bulk, which cause the generation of nonselective voids and hence the decline of solute rejection; (ii) a certain minimal thickness is indispensable (several times of the size of nanofillers), to remain the membrane defect-free, and hence prolong the transfer pathway.[19,20]

Because of the molecular-size level, superior affinity, controllable cavity diameter and easy modification, cyclodextrin (CD) seems an ideal candidate for use in OSN application. CD is a peculiarly torus-shaped biological supermolecule composed of a hydrophilic external surface and a hydrophobic cavity.[21−23] The cavity diameters of CD are in the range of 4.3−7.5 Å, and can allow small molecules to transport across.[24] Coincidently, the diameters of most nonpolar solvent molecules are in this range.[25] Therefore, CD may work as a nonpolar solvent pathway through its hydrophobic cavity, and the permeation ability can be tuned by adjusting the cavity size. In addition, the external surface of CD can be easily functionalized by diverse pendant groups, which regulate the free volume of polymer bulk via the interface interactions.[26] Actually, the combination of CDs within a polymer to form a composite membrane for water treatment has been widely studied.[27,28] However, studies of CDs in the OSN field lag behind, along the relevant literature, up to now. Therefore, it is rationally conjectured that tuning the cavity sizes of CD and free volume of the polymer matrix can elaborately manipulate the solvent transport properties of TFN OSN membranes.

Herein, a series of CDs with controllable cavity size and functional group (grafted on CD external surface) were employed to fabricate the TFN OSN membranes via interfacial polymerization for the first time. PEI was utilized as a polymer matrix due to its excellent chemical durability, good thermal and mechanical properties.[29,30] The CDs were dispersed into PEI solution and then dip-coated onto hydrolyzed polyacrylonitrile (PAN) ultrafiltration membrane. Within the active layer, the hydrophilic free volume cavities of PEI endowed the membrane with an efficient transport ability for a polar solvent. Meanwhile, the hydrophobic cavity of CD mainly allowed solvent molecules to get across, peculiarly enhancing the permeate fluxes of nonpolar solvents. In such a way, a dual-pathway architecture was constructed within the membrane. The size-controllable transfer behaviors of these two pathways were systematically investigated. The microstructures, physicochemical properties, and nanofiltration performances of the TFN membranes were investigated in detail. Moreover, the extended trial was also explored to evaluate the potential for practical application in OSN.

EXPERIMENTAL SECTION

Materials and Chemicals. PEI (Mw of 20 000 Da), trimesoyl chloride (TMC), sodium-*p*-styrenesulfonate (SSS), and 1-vinylimidazole (VIm) were purchased from Alfa Aesar. Polyethylene glycol (PEG, Mw values of 200, 400, 600, 800, 1000, and 2000 Da) oligomers and CDs (including α-CD, β-CD, and γ-CD) were obtained from Chengdu Xiya Reagent Research Center. Polystyrene (PS, Mw of 1000 Da) was supplied by Sigma-Aldrich. Sodium hydroxide was supplied by Guangfu Fine Chemical Research Institute. 2,2′-Azobis(isobutyronitrile) (AIBN) and acetonitrile were obtained from Kewei Chemistry Co., Ltd. Divinylbenzene (DVB, 80% divinylbenzene isomers) was provided as technical grade by Shengli Chemical Technical Faculty and was washed with 5% aqueous sodium hydroxide, then dried over anhydrous magnesium sulfate. 3-(Methacryloxy)propyltrimethoxysilan (MPS) and styrene (St) were purchased from Aldrich and distilled under vacuum. Isopropyl alcohol, hexane, *n*-heptane, and toluene were provided by Tianjin Kermel Chemistry Co., Ltd. PAN support with the molecular weight cutoff (MWCO) of 100 kDa was purchased from Shanghai MegaVision Membrane Engineering & Technology Co., Ltd. Deionized water was used throughout the experiments.

Surface Modification of the β-CDs. Surface modified β-CDs (β-CD-M) were synthesized via distillation−precipitation polymerization (Scheme 1).[31] The detailed procedure was as shown below (taking β-CD-SO_3H as an example): β-CD (5.0 g) was dispersed into the mixture of ethanol (180 mL), water (20 mL), and ammonium aqueous solution (25% w/w, 15 mL) with vigorous stirring at room temperature for 24 h. Afterward, excess MPS (1.0 mL) was added into the resultant mixture and stirred for another 24 h. The resulting mixture of alcosol β-CD and MPS was purified by three cycles of centrifugation (about 10000 rpm), decantation, and resuspended in ethanol with ultrasonic-bathing. Subsequently, MPS-modified β-CD was achieved by drying in a vacuum oven at 50 °C until constant weight.

Scheme 1. Synthetic Procedure of the β-CD-M through Distillation−Precipitation Polymerization

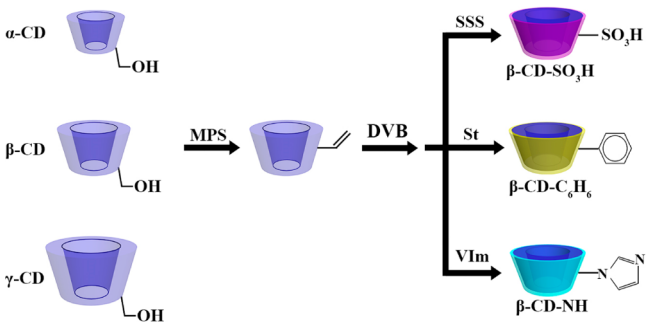

MPS-modified β-CD (0.30 g), monomer SSS (0.40 g), cross-linker DVB (0.50 mL), and initiator AIBN (0.02 g) were dissolved in acetonitrile (80 mL) in a dried two-necked flask. The above mixture was heated and kept under boiling state until 40 mL of acetonitrile was distilled out. After being purified and dried, the resultant SSS-modified β-CD was treated with 0.1 M HCl to exchange the Na^+ in $-SO_3Na$

DOI: 10.1021/acssuschemeng.5b00435
ACS Sustainable Chem. Eng. 2015, 3, 1925−1933

with H^+. Then, the β-CD bearing sulfonic acid groups (β-CD-SO_3H) was obtained after being dried in a 50 °C vacuum oven until a constant weight.[32] The β-CD bearing phenyl group (β-CD-C_6H_6) and imidazolyl group (β-CD-NH) on the external surface were prepared via a similar procedure, using St and VIm as the functional monomers, respectively.

Preparation of the Nanocomposite Membranes. A certain amount of PEI was dissolved into water by mechanical stirring for 0.5 h to form aqueous solution (4 wt %, 20 mL), where the CDs (1.5 wt % to PEI) were added into the above solution. An ultrasonic bath for about 1 h was conducted under the ice−water bath (around 0 °C) to ensure a uniform dispersion of CDs. Subsequently, the PEI/CD solution was dip-coated onto the top of the PAN support. After 10 min, the excess PEI/CD solution was removed to attain a thin active layer. Then, a hexane solution of TMC (2 wt %, 20 mL) was prepared under stirring for 1 h and then poured into the above-coated PAN support for another 10 min to perform the interfacial polymerization. The resulting TFN−CD membrane was dried in atmosphere for 1 h and then placed in a 60 °C drying cabinet for 4 h to make the cross-linking complete. The preparation process of the nanocomposite membrane is shown in Scheme S1 in detail. For simplicity, the as-obtained membranes were denoted as TFN−X-CD and TFN−β-CD-M, where X represented the type of CD (α, β, and γ) and M referred to the functional group (SO_3H, NH, and C_6H_6). It should be noted that for investigating the influence of CD loading amount, a series of TFN−β-CD membranes with the β-CD loading amount ranging from 0.5 to 3.0 wt % were prepared. Control membrane denoted as TFC was fabricated without embedding CD, for comparison.

Because of the severe interference of the PAN support, the data measured by the whole TFN−CD membrane could not accurately reflect the free volume of active layer. Therefore, the active layer was necessary to peel off for further analysis. The PEI−CD solutions were cast onto a Teflon plate, and then cross-linked by TMC to fabricate the free-standing active layers. The resultant membranes were peeled off after drying in a 60 °C drying cabinet for 24 h. Then, the as-prepared membranes were designated as PEI−X-CD and PEI−β-CD-M, where X represented the type of CD and M referred to the functional group.

Characterizations. Chemical structure of the CDs and membranes were characterized by Fourier transform infrared (FTIR, Nicolet MAGNA-IR 560) with a resolution of 4 cm^{-1} in the range of 4000−400 cm^{-1}. Thermal properties of the CDs and membranes were conducted by thermogravimetric analysis (TGA), which was performed on a TGA-50 SHIMADZU instrument operating from 25 to 800 °C with 10 °C min^{-1} under nitrogen atmosphere. Surface and cross section images of the membranes were observed by scanning electron microscopy (SEM, JSM7500F) after being freeze-fractured in liquid nitrogen; subsequently, the membranes were sputtered with Au by an ion sputtering instrument (JS-1600, Beijing Hetong MITTR Co., Ltd.) with a thickness about 10 nm under the vacuum degree of 5 Pa. The hydrophobic/hydrophilic nature of the membranes was determined by a contact angle goniometer (JC2000C Contact Angle Meter, Powereach Co.) at room temperature and at least 5 measurements were performed on each sample. Free volume characteristics (i.e., FFV and density) of the membranes were performed by a buoyancy method according to the literature, the standard deviations were obtained from an average of 3−4 membrane samples.[33,34] The detailed calculation process of FFV and membrane density is supplied in the Supporting Information.

Evaluation of Solvent Permeation and Rejection Properties. Solvent permeation and separation experiments were carried out by a N_2 pressurized dead-end unit provided with 5 cells connected in series (Scheme 2). The cell with the volume of 200 mL was equipped with a magnetic stirring about 300 rpm to weaken the concentration gradient. The membrane sample with the effective area of 18.0 cm^2 was fixed by an O-ring within the cell to seal. All the experiments were carried out under the 10 bar and 27 °C. Permeate flux and rejection curve of the membrane were performed to evaluate the membrane performance. Three organic solvents (e.g., *n*-heptane, isopropyl alcohol, and toluene) were used for experiment. Because of the invasion of organic solvent, the membrane would lose its original structure or keep its primitive shape. Therefore, the membrane samples were immersed in the pure solvent for at least 48 h to get entirely swelling equilibrium prior to the test.[35] After precompacting for 1 h, permeate fluxes of membrane samples were immediately collected at intervals of 1 h, whereas the rejections were taken once the operating time was reached (4 h). The obtained fluxes were higher than the steady state values. PEG oligomers (500 mg L^{-1}) were dissolved in isopropyl alcohol as feed solutions. The concentration of PEG in permeate solution was quantified using spectrophometic method. The PEG solution was colored by $BaCl_2/I_2$ and then scanned using ultraviolet spectrophotometry to draw the standard curve of the PEG solution (PEG concentration vs absorbance). Then, the amount of PEG in permeate solution was calculated by its absorbance according to the standard curve.[36] The detailed measurement of PEG for rejection is provided in the Supporting Information (Figure S9). Moreover, PS 1000 (500 mg L^{-1}) was dissolved in *n*-heptane and toluene as feed solutions, respectively. The quantitative analysis of PS 1000 in permeate and feed solutions was performed by an Agilent HPLC system.

Permeate flux (F, L m^{-2} h^{-1}) was calculated by the permeate volume (V, L) per unit area (A, m^2) per unit time (t, h) using eq 7:

$$F = \frac{V}{A \cdot t} \tag{7}$$

The rejection (R, %) was defined as eq 8, where C_P (mg L^{-1}) and C_F (mg L^{-1}) represented the solute concentrations in permeate and feed solutions, respectively.

$$R = \left(1 - \frac{C_P}{C_F}\right) \times 100 \tag{8}$$

The standard deviations of permeate flux and rejection were calculated from an average of 3−4 membranes with an error within ±4.3%.

Scheme 2. Schematic Representation of Filtration Unit[a]

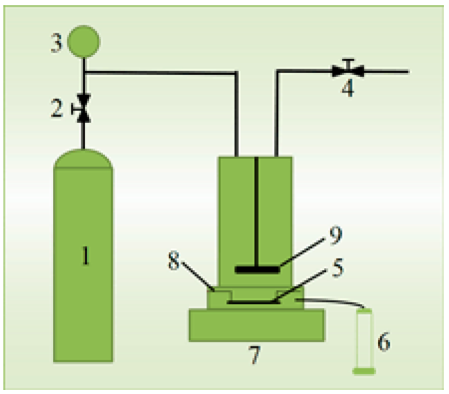

[a]1, nitrogen cylinder; 2, regulating valve; 3, pressure gauge; 4, decompression valve; 5, OSN membrane; 6, graduated cylinder; 7, magnetic stirrer; 8, sealing washer; 9, magnetic stick.

RESULTS AND DISCUSSION

In this study, a series of CDs with controllable cavity size and functional group were dispersed into the PEI matrix to fabricate TFN−CD membranes for OSN application. During the preparation, the same amount of PEI was utilized to ensure a close thickness for all the membranes. Within the active layer, the cavities of CDs were expected to serve as hydrophobic pathways for nonpolar solvents, whereas the free volume cavities of the PEI matrix might act as hydrophilic pathways for polar solvents. Therefore, the solvent permeation properties of the TFN−CD membranes would be elaborately manipulated

DOI: 10.1021/acssuschemeng.5b00435
ACS Sustainable Chem. Eng. 2015, 3, 1925−1933

Table 1. Basic Properties of X-CD

CD	no. glucose units	molecular weight	cavity diameter (Å)	cavity height (Å)	density (g cm^{-3})	decomposition temperature (°C)
α-CD	6	972	4.7−5.2	7.9	1.624	321.3
β-CD	7	1135	6.0−6.4	7.9	1.624	328.7
γ-CD	8	1297	7.5−8.3	7.9	1.624	321.0

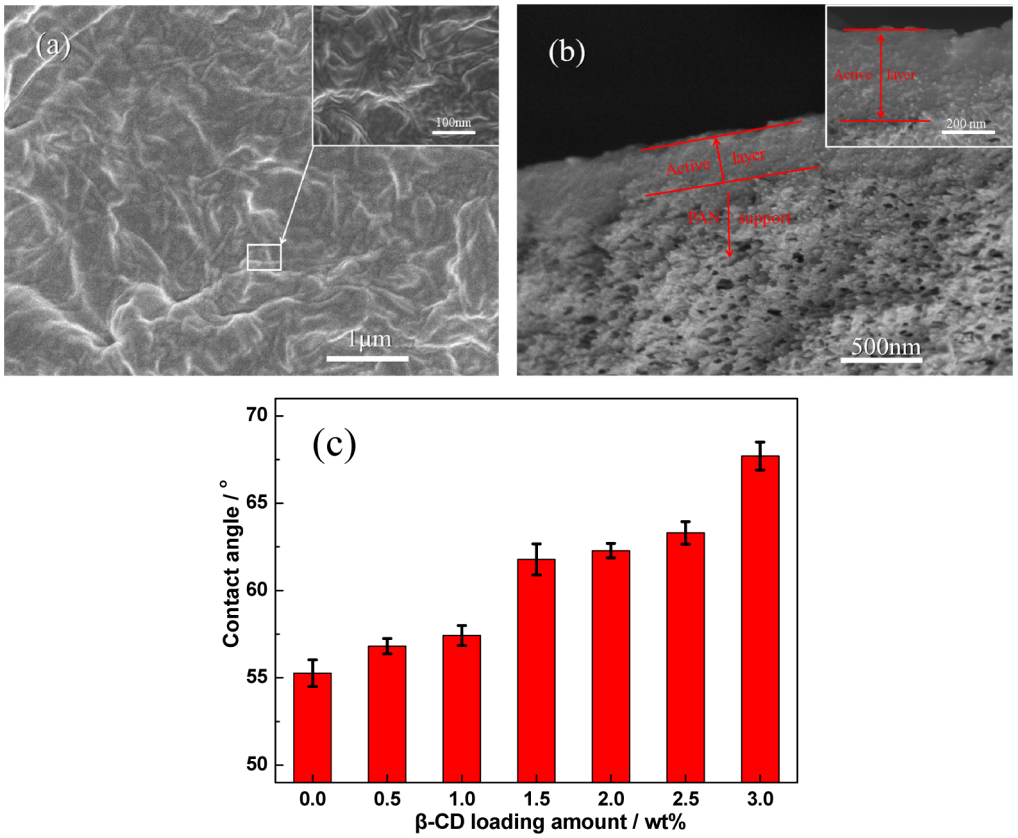

Figure 1. SEM images of the surface (a) and cross section (b) of TFN−β-CD, and (c) contact angle values of TFN−β-CD membranes with the β-CD loading amount ranging from 0.5 to 3.0 wt %.

by tuning the cavity size of CD and the free volume of PEI matrix.

Regulation and Performances of the Hydrophobic Pathways. It is well-known that the nanosized CD has a plenty of hydroxyls on its external surface, which affords hydrophobic nature to the cavity driven by cage effect. In this study, three commonly used X-CDs (i.e., α-CD, β-CD, and γ-CD) were utilized as the nanofillers, their detailed properties were summarized in Table 1.[25,37] The physicochemical properties of organic solvents used were supplied in Table S1. The X-CDs have similar chemical structure but different cavity size, and the diameters of the small mouths of α-CD, β-CD, and γ-CD are 0.47, 0.60, and 0.75 nm, respectively.

The morphologies of the as-obtained membranes were observed by SEM Figure 1a show the representative surface morphology of TFN−X-CD, which revealed that the active layer was equably deposited on the PAN support without obvious defects.[38] The contrast difference across the PAN support (Figure 1b) indicated the active layer was dense with an average thickness of 322 ± 12 nm, which was in agreement with the literature.[39] Further discussion about SEM images of the membranes can be found in Figure S1. The chemical structure and the incorporation of X-CDs of TFN−X-CD were confirmed by FTIR spectra (Figure S2). The surface hydrophobicty of membrane was measured in the form of contact angle, and the results are shown in Figure 1c. A contact angle of 55.3° was attained by TFC, suggesting a semihydrophilic nature of the PEI matrix.[13] By comparison, the incorporation of hydrophilic β-CD afforded the TFN−β-CD higher contact angle, i.e., a reduced hydrophilic nature. Moreover, increasing the β-CD loading amount from 0.5 to 3.0 wt % gradually elevated the contact angle from 56.8° to 67.7°. Such a phenomenon was probably attributed to the presence of X-CD upon the membrane surface, resulting in the hydrophobic cavity exposed in air. Primarily, the X-CD was randomly dispersed in PEI aqueous phase at first. During the interfacial polymerization, the hydrophobic cavity would tend to expose within the *n*-hexane phase driven by the forces from van der Waals and hydrophobic interactions.[40] In such a way, the hydrophobic cavity of X-CD might be exposed upon membrane surface, imparting an increase of contact angle for TFN−X-CD.

Previous studies have demonstrated that the transport mechanism of the OSN membrane obeys a solution-diffusion mechanism and/or pore flow mechanism. The transport ability of the solvent molecule is strongly determined by its molecular size. For the active layer, free volume characteristics can reflect the diffusion ability of the PEI matrix for an organic solvent.[10,41] As shown in Table 2, the membrane density and FFV of the

DOI: 10.1021/acssuschemeng.5b00435
ACS Sustainable Chem. Eng. 2015, 3, 1925−1933

Table 2. Densities and FFV Values of the Active Layers Determined by Buoyancy Method

active layer	ρ_B (g cm^{-3})	FFV (%)
PEI	0.678 ± 0.007	0.486 ± 0.005
PEI-α-CD	0.663 ± 0.008	0.500 ± 0.004
PEI-β-CD	0.662 ± 0.005	0.501 ± 0.003
PEI-γ-CD	0.664 ± 0.006	0.499 ± 0.006
PEI-β-CD-C_6H_6	0.661 ± 0.006	0.502 ± 0.002
PEI-β-CD-SO_3H	0.671 ± 0.003	0.494 ± 0.005
PEI-β-CD-NH	0.647 ± 0.008	0.512 ± 0.007

PEI were 0.678 g cm^{-3} and 0.486%, respectively. This high FFV confirmed that PEI chains formed network structures with the aid of the hydrogen-bonding interactions and cross-linking reaction. By comparison, PEI-X-CD attained lower density values (around 0.663 g cm^{-3}) and higher FFV values (around 0.5%) than those of the PEI active layer. Such a phenomenon was probably due to the insertion of X-CD within PEI networks, which enlarged the free volume by steric effects and interfacial interactions. Besides, the membrane density and FFV value for PEI-X-CD maintained a relatively stable constant. Such a phenomenon was probably attributed to the competitive relationships between the cavity size and specific surface area of X-CD.[42] Explicitly, a constant loading of X-CD was introduced into the dope solution to prepare the TFN−X-CD. Larger cavity size of X-CD endowed the resulting membrane with a higher FFV value; whereas as the increase of X-CD size, the specific surface area was gradually decreases, resulting in the lower FFV value. Considering the close free volume characteristics, the transport properties of TFN−X-CD membranes would be related to the change in the FFV value of the PEI matrix and the cavity size of X-CD.

The permeate fluxes of the as-obtained membranes are depicted in Figure 2a. The hydrophilic nature of PEI endowed the TFC with excellent transfer ability for isopropyl alcohol, the permeance of which was as high as 3.37 L m^{-2} h^{-1} bar $^{-1}$. Whereas, for the nonpolar solvents, the TFC exhibited a lower permeation ability, specifically, 0.45 L m^{-2} h^{-1} bar $^{-1}$ for *n*-heptane and 0.56 L m^{-2} h^{-1} bar $^{-1}$ for toluene. By comparison, the presence of X-CD altered the solvent permeation properties, and the detailed alterations were generalized as follows: (i) the incorporation of α-CD notably increased the permeance of *n*-heptane from 0.45 to 1.82 L m^{-2} h^{-1} bar $^{-1}$, whereas the permeances of isopropyl alcohol (from 3.37 to 2.71 L m^{-2} h^{-1} bar $^{-1}$) and toluene (from 0.56 to 0.5 L m^{-2} h^{-1} bar $^{-1}$) decreased; (ii) the incorporation of β-CD elevated the permeances of *n*-heptane and isopropyl alcohol up to 3.86 and 2.23 L m^{-2} h^{-1} bar $^{-1}$, respectively, while the permeance of toluene was below 0.13 L m^{-2} h^{-1} bar $^{-1}$; (iii) the incorporation of γ-CD gave a significant enhancement in the transfer ability for these three solvents, and the permeances were elevated to 3.94, 4.02, and 2.52 L m^{-2} h^{-1} bar $^{-1}$ for isopropyl alcohol, *n*-heptane, and toluene, respectively. Considering the close free volume characteristics for all the TFN−X-CD membranes, the effect of the varying FFV values of the PEI matrix on the membrane performance could be neutralized. Therefore, the transfer property of as-obtained membrane was mainly dependent on the cavity size of X-CD, as illustrated in Scheme 3: (i) the cavity of α-CD (0.47 nm) only allowed *n*-heptane (0.43 nm) to get through, whereas for the large-sized solvents (e.g., isopropyl alcohol and toluene) the α-CD would obstruct

Scheme 3. Schematic Illustration of the Transport Ability of X-CD Cavity for Solvent Molecules[a]

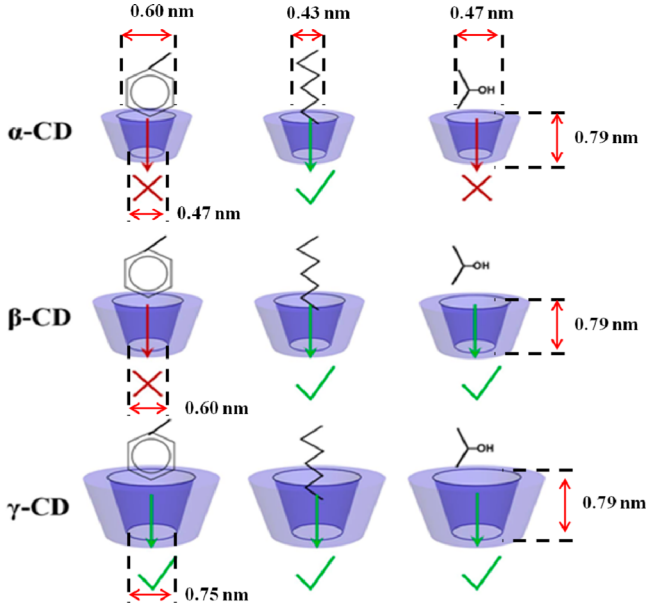

[a]The organic solvents (from left to right) were toluene, *n*-heptane, and isopropyl alcohol.

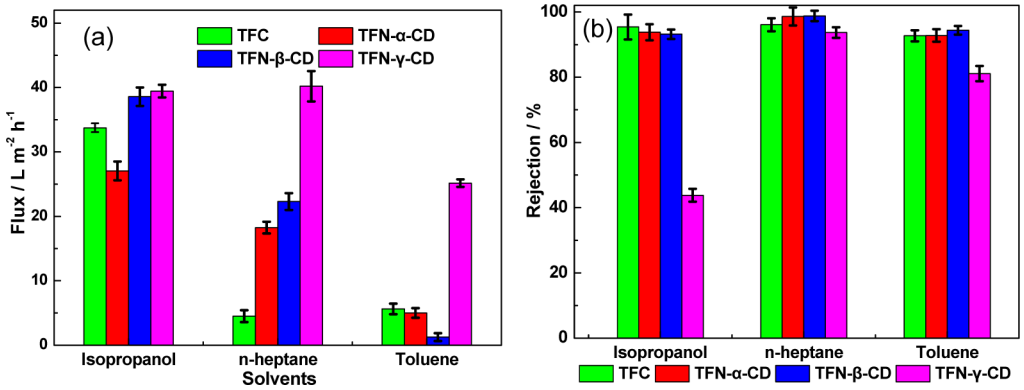

Figure 2. (a) Permeate fluxes of the TFN−X-CD for isopropyl alcohol, *n*-heptane, and toluene; (b) rejections of TFN−X-CD for filtrations of isopropyl alcohol with PEG 1000, and of *n*-heptane and toluene with PS 1000. The experiments were carried out at 10 bar and room temperature, and the X-CD loading amount was 1.5 wt %.

DOI: 10.1021/acssuschemeng.5b00435
ACS Sustainable Chem. Eng. 2015, 3, 1925−1933

its transfer pathway and thus raise their diffusion resistance; (ii) the cavity of β-CD (0.60 nm) could allow *n*-heptane (0.43 nm) and isopropyl alcohol (0.47 nm) to migrate across but not toluene (0.60 nm); (iii) the cavity of γ-CD (0.75 nm) could allow these three solvents to get across. The rejection abilities of TFN−X-CD were investigated using PEG 1000 (isopropyl alcohol) and PS 1000 (*n*-heptane and toluene) as solutes, as shown in Figure 2b. Figure S10 demonstrates the selectivity was driven by the active layer and not by the PAN support after the post-treatments. It was found that the rejection abilities of the composite membranes maintained almost unchanged with the incorporation of X-CD. For instance, the rejections of PEG 1000 or PS 1000 for TFC, TFN−α-CD, and TFN−β-CD were all above 93%. Nevertheless, the rejection of TFN−γ-CD for PEG 1000 in isopropyl alcohol was just 43.8%. Such a phenomenon was probably due to the larger cavity of γ-CD, which allowed the linear PEG transporting through the membrane. Meanwhile, the rejections of PS 1000 for TFN−X-CD in *n*-heptane were much higher than those in toluene, indicating the better affinity between the PS 1000 and toluene. In addition, the rejection curves of TFN−X-CD were conducted in isopropyl alcohol using PEG oligomers as solutes (see Figure S3). Explicitly, the presence of α-CD and β-CD obstructed and lengthened the diffusion pathway for PEG oligomers, thus donating enhanced rejection abilities to the TFN membranes. For instance, the MWCOs of TFN−α-CD, TFN−β-CD were 263 and 337, respectively, lower than the 709 of TFC.[43] For comparison, a commercial integrally skinned asymmetric OSN membrane (STARMEMt122, UK) was measured with the same experimental equipment, which attained the *n*-heptane permeance of 0.08 L m^{-2} h^{-1} bar^{-1}. Therefore, the TFN−CD possessed an acceptable permeation ability, for instance, the *n*-heptane permeance of TFN−β−CD was 2.23 L m^{-2} h^{-1} bar^{-1}. According to the above results, a controllable pathway for solvent transport was constructed with the help of X-CD and PEI matrix within TFN membrane, especially for nonpolar solvents.

The number and continuousness of this pathway could be facilely tuned by the CD loading amount. Transport abilities of the membrane for organic solvent was investigated by three solvents, containing *n*-heptane, isopropyl alcohol, and toluene, whereas the rejection ability of the membrane was measured by PEG 1000 as a solute in isopropyl alcohol.[36] Figure 3 clearly reveals that the isopropyl alcohol and *n*-heptane fluxes increased almost linearly with the β-CD loading amount increasing from 0.5 to 2.0 wt %, due to the increase of CD-based transfer pathways. When the β-CD loading amount is further increased from 2.0 to 3.0 wt %, a soaring increase in isopropyl alcohol and *n*-heptane fluxes was observed, probably due to the regional agglomeration of β-CD caused by the high surface tension and the hydrophobic interactions. As discussed above, because toluene could not transport through the cavity of β-CD, the toluene flux decreased gradually with the increase of β-CD loading amount from 0.5 to 3.0 wt %. It should also be noted that the rejection for PEG 1000 decreased slightly from 99.2% to 98.9% when the β-CD loading amount was elevated from 0.5 to 1.5 wt %, whereas it declined from 89.8% to 42.6% when the loading amount varied from 2.0 to 3.0 wt %. The sharp decrease of rejection was probably due to the agglomeration of β-CD, which formed nonselective voids for PEG transport.[44] Moreover, the rejection of PEG 1000 decreased gradually with the increase of β-CD loading amount. This finding indicated that the permeability of PEG 1000 for

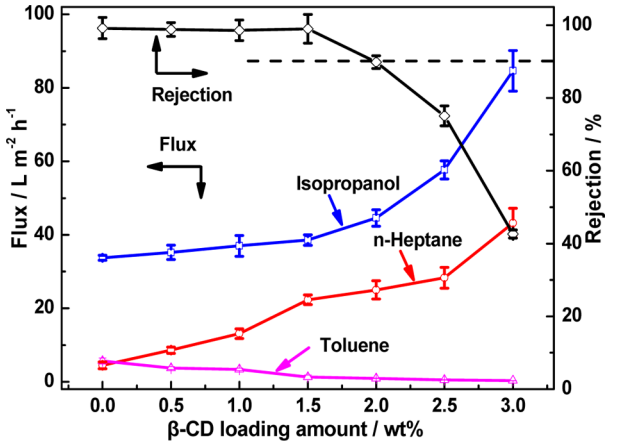

Figure 3. Isopropyl alcohol, *n*-heptane, and toluene fluxes of TFN−β-CD with different CD loading amounts and the corresponding rejections of PEG 1000 in isopropyl alcohol under 10 bar and room temperature.

TFN-β-CDs was increased compared with the TFC, probably resulting from the formation of defects. Considering the comprehensive performance, 1.5 wt % CD loading was employed responsibly to survey the effects of the cavity size and functional group on the transfer properties of membrane.

Regulation and Performances of the Hydrophilic Pathways. In the previous section, unique pathways constructed by X-CD could efficiently transport a nonpolar solvent. For another, the free volume cavities of PEI matrix could work as hydrophilic pathways due to the presence of abundant hydrophilic-bonding sites, which mainly allowed polar solvent to get through. Many efforts have been devoted to regulating the free volume characteristics of the membrane.[45,46] Among them, one convenient and efficient strategy was to regulate the interfacial interactions between polymer and nanofillers. Herein, β-CD was chosen as representative and then modified with three functional groups on its external surface for regulating the interfacial interactions with PEI chains. The presence of the functional groups (i.e., sulfonic acid, phenyl group, and imidazolyl group) was confirmed by FTIR spectra and TGA results (Figures S4 and S5), which might provide the possibility to manipulate the membrane microstructures and performances.

Membrane density and FFV values presented in Table 2 were employed to assess the free volume characteristics of the membrane. Compared with the density (0.662 g cm^{-3}) and FFV (0.496%) of PEI-β-CD, it was found that PEI-β-CD-C_6H_6 displayed a similar density (0.661 g cm^{-3}) and FFV (0.497%). PEI-β-CD-SO_3H attained an increased density of about 0.671 g cm^{-3} and a reduced FFV of about 0.489%. In contrast, PEI-β-CD-NH possessed an elevated FFV of about 0.502% and a reduced density of about 0.647 g cm^{-3}. Such phenomena were probably due to the variations of mutual interactions at PEI/β-CD-M interfaces, and the possible models are illustrated in Scheme S2. Case I represented the interface morphology of TFN−β-CD-SO_3H, in which strong electrostatic attractions were generated between PEI chains and β-CD-SO_3H. These attractions could inhibit the motion of PEI chains and thus lead to a dense and compact chain stacking, affording the reduced FFV and increased density.[47] Case II denoted the interface morphology of TFN−β-CD-NH. Contrast to the interactions in Case I, electrostatic repulsions would emerge due to the

DOI: 10.1021/acssuschemeng.5b00435
ACS Sustainable Chem. Eng. 2015, 3, 1925−1933

protonation of $-NH_2/NH-$ in PEI and imidazole in β-CD-NH. The repulse force would suppress the hydrogen-bonding interactions among PEI chains and then disrupt the intrinsic chain packing. Consequently, the PEI networks became loose near the β-CD-NH interface, resulting in the reduced density and increased FFV. Case III represented the situation in TFN−β-CD-C_6H_6, which possessed close free volume characteristics to those of TFN−β-CD. In this case, there was no obvious interaction between PEI chains and β-CD-C_6H_6, and therefore the chain packing of PEI was slightly altered. The hydrophobic/hydrophilic nature of TFN−β-CD-M was also probed, as shown in Figure S6. By comparison, the contact angles of TFN−β-CD-NH and TFN−β-CD-SO_3H were reduced to 59.5° and 53.9°, respectively, whereas the contact angle of TFN−β-CD-C_6H_6 was increased to 69.5° in comparison with the 61.8° of TFN−β-CD. Coincidentally, such findings were consistent with the hydrophilic/hydrophobic properties of the introduced β-CD-M, that is, the hydrophilic nature of β-CD-NH and β-CD-SO_3H and the hydrophobic nature of β-CD-C_6H_6. A similar observation has been reported in other literature.[10,19]

Considering the acceptable solvent permeation ability of TFN−β-CD, isopropyl alcohol and *n*-heptane were employed to probe the membrane performances of TFN−β-CD-M, as depicted in Figure 4. As the diffusion of molecules mainly took

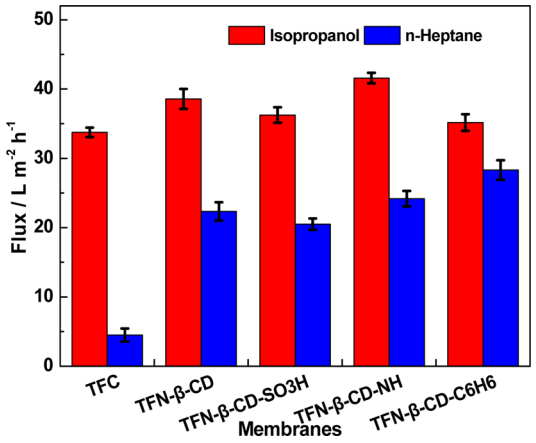

Figure 4. Isopropyl alcohol and *n*-heptane fluxes of TFN−β-CD-M under 10 bar and room temperature. The β-CD-M loading amount was 1.5 wt %.

place in the free volume cavities of the polymer matrix, the more and larger free volume cavities would confer a higher transport rate on the membrane. Exemplarily, the isopropyl alcohol fluxes of TFN−β-CD-M clearly verified the correlation between the FFV values and the transport properties. Specifically, in Case I, the addition of β-CD-SO_3H decreased the free volume cavities, which resulted in a lower isopropyl alcohol permeance (3.62 L m^{-2} h^{-1} bar^{-1}) than that of TFN−β-CD (3.86 L m^{-2} h^{-1} bar^{-1}). The reduced cavities and inhibited chain motion increased the migration resistance for isopropyl alcohol. By comparison, the presence of β-CD-NH enlarged the free volume cavities of TFN−β-CD-NH (Case II), conferring a higher isopropyl alcohol permeance (4.16 L m^{-2} h^{-1} bar^{-1}) when compared with that of TFN−β-CD. In Case III, although TFN−β-CD-C_6H_6 possessed similar free volume characteristics to those of TFN−β-CD, the strong hydrophobic nature of TFN−β-CD-C_6H_6 might suppress the solution of hydrophilic isopropyl alcohol. Consequently, TFN−β-CD-C_6H_6 had a lower permeance (3.52 L m^{-2} h^{-1} bar^{-1}) than that of TFN−β-CD. The *n*-heptane fluxes of TFN−β-CD-SO_3H and TFN−β-CD-NH displayed the similar trend to that of isopropyl alcohol flux. Such observations suggested that the higher the FFV value was, the faster solvent transported through the membrane. In addition, the *n*-heptane fluxes of TFN−β-CD-M also confirmed the relationship between the contact angle and the transport properties. With the addition of hydrophilic β-CD-NH or β-CD-SO_3H, the contact angle of the relevant membrane was reduced, affording the lower *n*-heptane flux. The TFN−β-CD-C_6H_6 possessed the higher contact angle, which acquired the highest *n*-heptane permeance of 2.83 L m^{-2} h^{-1} bar^{-1} among the membranes. Such an observation corroborated that the hydrophobic/hydrophilic nature of the membranes had an important influence on the membrane performance. The rejection ability of TFN−β-CD-M was higher than that of TFC, and it changed slightly varying with the functional groups on β-CD-M (Figure S7). The MWCOs of TFN−β-CD-M varied from 324 to 374 g mol^{-1}. This finding implied that the morphology regulation at the PEI-β-CD interfacial domains had weak influence on the transport ability of the large-sized solute. Accordingly, these results clearly demonstrated that tuning the free volume cavities of the PEI matrix and hydrophobic/hydrophilic properties could efficiently manipulate the transport properties of the membrane, particularly for polar solvents.

Extended Trial of the Membrane. TFN−β-CD-NH was chosen as representative for the investigation of operational stability. Figure 5 illustrates the time-dependent flux and

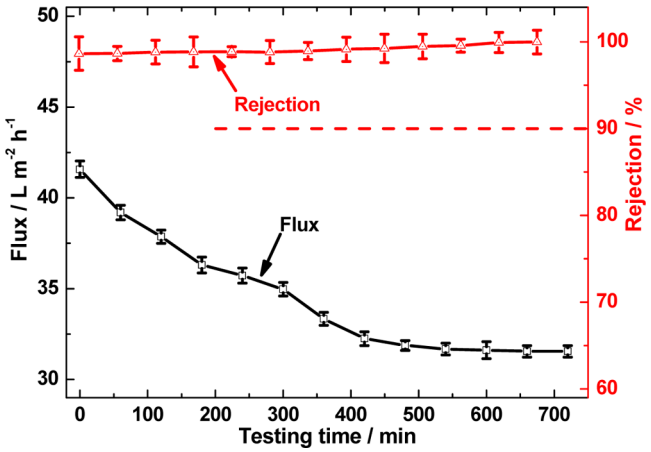

Figure 5. Extended OSN trial of TFN−β-CD-NH in isopropyl alcohol solution using PEG 1000 as solute under 10 bar and room temperature. The β-CD-NH loading amount was 1.5 wt %.

rejection of TFN−β-CD-NH for 720 min. It could be found that during the beginning 420 min, the permeance of isopropyl alcohol decreased from 4.16 to 3.23 L m^{-2} h^{-1} bar^{-1} with a reduction of 22.4%. Such reduction was rationally ascribed to the compaction of membrane and the pore blockage by solvent molecules. After this period, the membrane reached a stable transport state, and the permeance kept almost the constant value of 3.16 L m^{-2} h^{-1} bar^{-1}. Moreover, TFN−β-CD-NH possessed a high rejection around 99.3% for PEG 1000, and it only slightly altered during the whole test. Similar observations have been reported in other literatures.[10,20,48] Despite the flux

DOI: 10.1021/acssuschemeng.5b00435
ACS Sustainable Chem. Eng. 2015, 3, 1925−1933

reduction, the as-prepared membranes displayed potential operational stability for OSN application.

CONCLUSIONS

In summary, a series of novel TFN membranes with tunable solvent permeation properties were designed and fabricated via interfacial polymerization for organic solvent nanofiltration. Within the active layer, versatile CDs with controllable cavity size and functional group were incorporated into the PEI matrix. Through the systematical characterizations and measurements, it was found that distinct dual-pathways were constructed via this facile method: (i) the cavities of CDs formed efficient and fast pathways to transport organic solvent (especially for nonpolar solvent), and the transport ability of the membrane could be accurately tuned by the cavity size of CD; (ii) the free volume cavities in the PEI matrix and hydrophobic/hydrophilic properties could efficiently manipulate the solvent permeation properties, particularly for polar solvents. In the latter case, the physicochemical properties of the membrane (FFV and contact angle) were regulated in virtue of the corresponding interfacial interactions and the surface functional groups. The as-prepared membranes achieved enhanced rejection ability and adequate operational stability for OSN application. The facile and generic strategy depicted herein might pave the way to understand better the regulation of membrane microstructures and then to design membrane with tunable transfer properties for the separation and purification, especially for the mixed organic solvents.

ASSOCIATED CONTENT

Supporting Information

The Supporting Information is available free of charge on the ACS Publications website at DOI: 10.1021/acssuschemeng.5b00435.

Calculation of fractional free volume and possible interface morphology, contact angle, SEM images, FTIR spectra, TGA and rejection curves of the as-prepared membranes, as well as the physicochemical properties of organic solvents (PDF).

AUTHOR INFORMATION

Corresponding Author

*J. Wang. E-mail: jingtaowang@zzu.edu.cn. Tel. (Fax): +86-371-63887135.

Notes

The authors declare no competing financial interest.

ACKNOWLEDGMENTS

We gratefully acknowledge financial supports from National Natural Science Foundation of China (21206151 and U1407121) and China Postdoctoral Science Foundation (2014T70687).

REFERENCES

(1) Marchetti, P.; Solomon, M. F. J.; Szekely, G.; Livingston, A. G. Molecular separation with organic solvent nanofiltration: a critical review. *Chem. Rev.* **2014**, *114*, 10735−10806.

(2) Liu, G. P.; Wei, W.; Jin, W. Q. Pervaporation membranes for biobutanol production. *ACS Sustainable Chem. Eng.* **2014**, *2*, 546−560.

(3) Chen, Y.; Jia, M. L.; Xu, H.; Cao, Y.; Fan, H. J. Counterintuitive gas transport through polymeric nanocomposite membrane: Insights from molecular dynamics simulations. *J. Phys. Chem. C* **2014**, *118*, 28179−28188.

(4) Figoli, A.; Marino, T.; Simone, S.; Di Nicolo, E.; Li, X. M.; He, T.; Tornaghi, S.; Drioli, E. Towards non-toxic solvents for membrane preparation: a review. *Green Chem.* **2014**, *16*, 4034−4059.

(5) Szekely, G.; Jimenez-Solomon, M. F.; Marchetti, P.; Kim, J. F.; Livingston, A. G. Sustainability assessment of organic solvent nanofiltration: from fabrication to application. *Green Chem.* **2014**, *16*, 4440−4473.

(6) Darvishmanesh, S.; Firoozpour, L.; Vanneste, J.; Luis, P.; Degreve, J.; Van der Bruggen, B. Performance of solvent resistant nanofiltration membranes for purification of residual solvent in the pharmaceutical industry: experiments and simulation. *Green Chem.* **2011**, *13*, 3476−3483.

(7) Vanneste, J.; Ormerod, D.; Theys, G.; Van Gool, D.; Van Camp, B.; Darvishmanesh, S.; Van der Bruggen, B. Towards high resolution membrane-based pharmaceutical separations. *J. Chem. Technol. Biotechnol.* **2013**, *88*, 98−108.

(8) Darvishmanesh, S.; Robberecht, T.; Luis, P.; Degreve, J.; Van der Bruggen, B. Performance of nanofiltration membranes for solvent purification in the oil industry. *J. Am. Oil Chem. Soc.* **2011**, *88*, 1255−1261.

(9) Darvishmanesh, S.; Degreve, J.; Van der Bruggen, B. Mechanisms of solute rejection in solvent resistant nanofiltration: the effect of solvent on solute rejection. *Phys. Chem. Chem. Phys.* **2010**, *12*, 13333−13342.

(10) Vandezande, P.; Gevers, L. E. M.; Vankelecom, I. F. J. Solvent resistant nanofiltration: separating on a molecular level. *Chem. Soc. Rev.* **2008**, *37*, 365−405.

(11) Loh, X. X.; Sairam, M.; Steinke, J. H. G.; Livingston, A. G.; Bismarck, A.; Li, K. Polyaniline hollow fibres for organic solvent nanofiltration. *Chem. Commun.* **2008**, *47*, 6324−6326.

(12) Peng, F. B.; Lu, L. Y.; Sun, H. L.; Wang, Y. Q.; Liu, J. Q.; Jiang, Z. Y. Hybrid organic−inorganic membrane: solving the tradeoff between permeability and selectivity. *Chem. Mater.* **2005**, *17*, 6790−6796.

(13) Darvishmanesh, S.; Degreve, J.; Van der Bruggen, B. Mechanisms of solute rejection in solvent resistant nanofiltration: the effect of solvent on solute rejection. *Phys. Chem. Chem. Phys.* **2010**, *12*, 13333−13342.

(14) Peyravi, M.; Jahanshahi, M.; Rahimpour, A.; Javadi, A.; Hajavi, S. Novel thin film nanocomposite membranes incorporated with functionalized TiO2 nanoparticles for organic solvent nanofiltration. *Chem. Eng. J.* **2014**, *241*, 155−166.

(15) Shao, L.; Cheng, X.; Wang, Z.; Ma, J.; Guo, Z. Tuning the performance of polypyrrole-based solvent-resistant composite nanofiltration membranes by optimizing polymerization conditions and incorporating graphene oxide. *J. Membr. Sci.* **2014**, *452*, 82−89.

(16) Vanherck, K.; Aerts, A.; Martens, J.; Vankelecom, I. F. J. Hollow filler based mixed matrix membranes. *Chem. Commun.* **2010**, *46*, 2492−2494.

(17) Vandezande, P.; Li, X.; Gevers, L. E. M.; Vankelecom, I. F. J. High throughput study of phase inversion parameters for polyimide-based SRNF membranes. *J. Membr. Sci.* **2009**, *330*, 307−318.

(18) Liu, W.; Li, Y.; Meng, X.; Liu, G.; Hu, S.; Pan, F.; Wu, H.; Jiang, Z.; Wang, B.; Li, Z.; Cao, X. Embedding dopamine nanoaggregates into a poly(dimethylsiloxane) membrane to confer controlled interactions and free volume for enhanced separation performance. *J. Mater. Chem. A* **2013**, *1*, 3713−3723.

(19) Sorribas, S.; Gorgojo, P.; Téllez, C.; Coronas, J.; Livingston, A. G. High flux thin film nanocomposite membranes based on MOFs for organic solvent nanofiltration. *J. Am. Chem. Soc.* **2013**, *135*, 15201−15208.

(20) Liu, W.; Hu, S.; Liu, G.; Pan, F.; Wu, H.; Jiang, Z.; Wang, B.; Li, Z.; Cao, X. Creation of hierarchical structures within membranes by incorporating mesoporous microcapsules for enhanced separation performance and stability. *J. Mater. Chem. A* **2014**, *2*, 5267−5279.

DOI: 10.1021/acssuschemeng.5b00435
ACS Sustainable Chem. Eng. 2015, 3, 1925−1933

(21) Harada, A.; Takashima, Y.; Nakahata, M. Supramolecular polymeric materials via cyclodextrin−guest interactions. *Acc. Chem. Res.* **2014**, *47*, 2128−2140.
(22) Crini, G. Review: a history of cyclodextrins. *Chem. Rev.* **2014**, *114*, 10940−10975.
(23) Yang, H.; Yuan, B.; Zhang, X. Supramolecular chemistry at interfaces: host−guest interactions for fabricating multifunctional biointerfaces. *Acc. Chem. Res.* **2014**, *47*, 2106−2115.
(24) Chen, P.; Liang, H. W.; Lv, H. X.; Zhu, H. Z.; Yao, H. B.; Yu, S. H. Carbonaceous nanofiber membrane functionalized by beta-cyclodextrins for molecular filtration. *ACS Nano* **2011**, *5*, 5928−5935.
(25) Szejtli, J. Introduction and general overview of cyclodextrin chemistry. *Chem. Rev.* **1998**, *98*, 1743−1753.
(26) Harada, A.; Kobayashi, R.; Takashima, Y.; Hashidzume, A.; Yamaguchi, H. Macroscopic self-assembly through molecular recognition. *Nat. Chem.* **2011**, *3*, 34−37.
(27) Malinga, S. P.; Arotiba, O. A.; Krause, R. W. M.; Mapolie, S. F.; Diallo, M. S.; Mamba, B. B. Cyclodextrin-dendrimer functionalized polysulfone membrane for the removal of humic acid in water. *J. Appl. Polym. Sci.* **2013**, *130*, 4428−4439.
(28) Adams, F. V.; Nxumalo, E. N.; Krause, R. W. M.; Hoek, E. M. V.; Mamba, B. B. Application of polysulfone/cyclodextrin mixed-matrix membranes in the removal of natural organic matter from water. *Phys. Chem. Earth* **2014**, *67−69*, 71−78.
(29) Wu, D. H.; Huang, Y. F.; Yu, S. C.; Lawless, D.; Feng, X. S. Thin film composite nanofiltration membranes assembled layer-by-layer via interfacial polymerization from polyethylenimine and trimesoyl chloride. *J. Membr. Sci.* **2014**, *472*, 141−153.
(30) Li, M. M.; Xu, J.; Chang, C. Y.; Feng, C. C.; Zhang, L. L.; Tang, Y. Y.; Gao, C. J. Bioinspired fabrication of composite nanofiltration membrane based on the formation of DA/PEI layer followed by cross-linking. *J. Membr. Sci.* **2014**, *459*, 62−71.
(31) Liu, G.; Zhang, H.; Yang, X.; Wang, Y. Facile synthesis of silica/polymer hybrid microspheres and hollow polymer microspheres. *Polymer* **2007**, *48*, 5896−5904.
(32) Yang, M.; Ma, J.; Zhang, C.; Yang, Z.; Lu, Y. General synthetic route toward functional hollow spheres with double-shelled structures. *Angew. Chem., Int. Ed.* **2005**, *44*, 6727−6730.
(33) Murali, R. S.; Sridhar, S.; Sankarshana, T.; Ravikumar, Y. V. L. Gas permeation behavior of Pebax-1657 nanocomposite membrane incorporated with multiwalled carbon nanotubes. *Ind. Eng. Chem. Res.* **2010**, *49* (49), 6530−6538.
(34) Li, Y.; Xin, Q.; Wu, H.; Guo, R.; Tian, Z.; Liu, Y.; Wang, S.; He, G.; Pan, F.; Jiang, Z. Efficient CO_2 capture by humidified polymer electrolyte membranes with tunable water state. *Energy Environ. Sci.* **2014**, *7*, 1489−1499.
(35) Darvishmanesh, S.; Degreve, J.; Van der Bruggen, B. Performance of solvent-pretreated polyimide nanofiltration membranes for separation of dissolved dyes from toluene. *Ind. Eng. Chem. Res.* **2010**, *49*, 9330−9338.
(36) Zhang, H.; Mao, H.; Wang, J.; Ding, R.; Du, Z.; Liu, J.; Cao, S. Mineralization-inspired preparation of composite membranes with polyethyleneimine−nanoparticle hybrid active layer for solvent resistant nanofiltration. *J. Membr. Sci.* **2014**, *470*, 70−79.
(37) Kakuta, T.; Takashima, Y.; Nakahata, M.; Otsubo, M.; Yamaguchi, H.; Harada, A. Preorganized hydrogel: self-healing properties of supramolecular hydrogels formed by polymerization of host guest-monomers that contain cyclodextrins and hydrophobic guest groups. *Adv. Mater.* **2013**, *25*, 2849−2853.
(38) Hermans, S.; Marien, Ha.; Van Goethem, C.; Vankelecom, I. F. J. Recent developments in thin film (nano)composite membranes for solvent resistant nanofiltration. *Curr. Opin. Chem. Eng.* **2015**, *8*, 45−54.
(39) Vicinanza, N.; Svenum, I. H.; Naess, L. N.; Peters, T. A.; Bredesen, R.; Borg, A.; Venvik, H. J. Thickness dependent effects of solubility and surface phenomena on the hydrogen transport properties of sputtered Pd77%Ag23% thin film membranes. *J. Membr. Sci.* **2015**, *476*, 602−608.
(40) Chao, W. C.; Huang, Y. H.; Hung, W. S.; An, Q.; Hu, C. C.; Lee, K. R.; Lai, J. Y. Effect of the surface property of poly(tetrafluoroethylene) support on the mechanism of polyamide active layer formation by interfacial polymerization. *Soft Matter* **2012**, *8*, 8998−9004.
(41) Sherwood, T. K.; Brian, P. L. T.; Fisher, R. E.; Dresner, L. Salt concentration at phase boundaries in desalination by reverse osmosis. *Ind. Eng. Chem. Fundam.* **1965**, *4*, 113−118.
(42) Ellouze, F.; Amar, N. B.; Mokhtar, M. N.; Zimmermann, W.; Deratani, A. Fractionation of homologous CD_6 to CD_{60} cyclodextrin mixture by ultrafiltration and nanofiltration. *J. Membr. Sci.* **2011**, *374*, 129−137.
(43) Zhang, H.; Zhang, Y.; Li, L.; Zhao, S.; Ni, H.; Cao, S.; Wang, J. Cross-linked polyacrylonitrile/polyethyleneimine-polydimethylsiloxane composite membrane for solvent resistant nanofiltration. *Chem. Eng. Sci.* **2014**, *106*, 157−166.
(44) Wu, H.; Tang, B. B.; Wu, P. Preparation and characterization of anti-fouling β-cyclodextrin/polyester thin film nanofiltration composite membrane. *J. Membr. Sci.* **2013**, *428*, 301−308.
(45) Chae, H. R.; Lee, J.; Lee, C. H.; Kim, I. C.; Park, P. K. Graphene oxide-embedded thin-film composite reverse osmosis membrane with high flux, anti-biofouling, and chlorine resistance. *J. Membr. Sci.* **2015**, *483*, 128−135.
(46) Shao, L.; Cheng, X.; Wang, Z.; Ma, J.; Guo, Z. Tuning the performance of polypyrrole-based solvent-resistant composite nanofiltration membranes by optimizing polymerization conditions and incorporating graphene oxide. *J. Membr. Sci.* **2014**, *452*, 82−89.
(47) Wang, J.; Zhang, H.; Jiang, Z.; Yang, X.; Xiao, L. Tuning the performance of direct methanol fuel cell membranes by embedding multifunctional inorganic submicrospheres into polymer matrix. *J. Power Sources* **2009**, *188*, 64−74.
(48) Ahmadiannamini, P.; Li, X.; Goyens, W.; Joseph, N.; Meesschaert, B.; Vankelecom, I. F. J. Multilayered polyelectrolyte complex based solvent resistant nanofiltration membranes prepared from weak polyacids. *J. Membr. Sci.* **2012**, *394*, 98−106.

DOI: 10.1021/acssuschemeng.5b00435
ACS Sustainable Chem. Eng. 2015, 3, 1925−1933